A Stochastic source model for the 2015 M_w 7.9 Gorkha, Nepal, Earthquake using Multi-Dimensional Ensemble Empirical Mode Decomposition technique

S Sangeetha[1], and *S.T.G* Raghukanth[2]

[1]Research scholar, Department of Civil Engineering, Indian Institute of Technology Madras, Chennai 600036, India.
[2]Associate professor, Department of Civil Engineering, Indian Institute of Technology Madras, Chennai 600036, India.

Abstract. The present study aims at developing a new strategy to model the spatial variability of slip on the rupture plane using multi-dimensional ensemble empirical mode decomposition (MEEMD) technique. Here, the earthquake slip distribution is split into finite number of empirical modes of oscillation called the intrinsic mode functions (IMFs). This help in identifying the fluctuation component and trend in the slip data. The trend is positive and characterizes the nonstationary mean of the slip distribution. The fluctuation component can be modelled as a stationary random field using an exponential power spectral density function. The trend can be modeled as an elliptic patch. This new technique is demonstrated for the slip distribution of the recent Nepal Earthquake, 2015. It is observed that the new model can be used to simulate the spatial complexity of slip distribution of any earthquake.

1 Introduction

Finite-fault inversion provides a key to understand the earthquake source complexities which is essential to predict realistic ground motion for a scenario earthquake. The derived finite-fault rupture models from inversion contain information on fluctuations of slip on the rupture plane. In addition, these earthquake slip distributions are inherently nonstationary due to the fact that slip vanishes towards the buried edges of the fault. This clearly states the level of complexity which cannot be modelled by simple deterministic functions. In such situations, stochastic approaches provide an alternate for characterizing the spatial complexity of slip on the rupture plane. Research has been carried along this direction, over the last two decade (Somerville *et al.,* Mai and Beroza, Lavallée *et al.*, Raghukanth and Iyengar, Raghukanth, Raghukanth and Sangeetha [1-6]). The method for investigating earthquake slip distribution in these works are based on stationary random processes models with Gaussian properties. Limitation with these studies are, the developed models are based on Fourier analysis. But, it is well known that the PSD exists if and only if the signal is a wide-sense stationary process. For nonstationary process PSD does not exist. In such situations, Fourier-based spectral analysis which uses sine and cosine functions as the basis, in analyzing nonlinear and nonstationary data can yield distorted and incomplete information on the nature of the nonstationary slip distribution.

Huang *et al.* [7] pointed out that the only way to represent the physics of nonlinear and nonstationary processes is through adaptive basis functions. They have demonstrated the superiority of Empirical mode decomposition technique (EMD) technique to others by analysing wind speed, tidal velocity and earthquake data. The technique has been previously applied to understand strong motion data of past earthquakes (Huang *et al*., Loh *et al*., Zhang *et al*., Raghukanth and Sangeetha [8-11]). Mallikarjuna *et al.* [12] has used the EMD approach to forecast the air traffic by modelling the fluctuation part using artificial neural network (ANN) technique and the trend through simple regression analysis. Raghukanth [5] has proposed a new data-driven technique, namely Bi-dimensional empirical mode decomposition (BEMD) to characterize earthquake slip distribution of past earthquakes. Here the slip distribution is modelled as a sum of fluctuation and trend component. The fluctuation component is simulated as an exponential random field. The shortcoming with this work is that modelling of the trend component has not been explored in detail. The trend component is deterministic for a particular earthquake, hence it has to be modelled as 2D nonstationary function and cannot be taken as mean value of trend part as considered in Raghukanth [5]. In this study, an attempt has been made to model the trend of the slip data.

* Corresponding author: ssangee.civil@gmail.com

2 Source model of Nepal earthquake, 2015

The 25th April 2015 (M_w 7.9) earthquake triggered many broadband instruments across the globe. Researchers have reported this event as the largest to have occurred in the Nepal region in the last eight decade. A multitude of inversion studies have been carried out (Hayes *et al.*, Yagi and Okuwaki, Lay *et al.*, Tung and Masterlark, Yue *et al.*, Zhang *et al.*, McNamara *et al.*, [13-19]) using seismological (teleseismic and strong motion) and geodetic (high-rate GPS, static GPS, InSAR,ALOS-2) observations of both the mainshock and its largest aftershock. Nevertheless, we restrict our study to the modelling and analysis of finite fault slip model proposed by Yagi and Okuwaki [14] (see Figure 1). The source model indicates a north dipping low-angled thrust fault in MCT with strike/dip/rake angle of 285/10/58.6. It can also be observed from the figure that the rupture extends about 160km along the strike and 88km along the dip direction with an average rupture velocity of 3km/s. A maximum slip of about 7.5m is concentrated at a radial distance of 50km to the east of epicentre (28.147 °N lat, 84.708°E long). The total seismic moment is 9.1 × 10^{20} Nm corresponding to M_w 7.9. The focal depth and depth to the top of fault are 15km and 4.58km respectively. The hypocentre of the event is located at a distance of 140 and 60km along the strike and dip directions, respectively. Rise time, which is defined as the time taken by each subfault to rupture completely is 0.8s while the source duration is 50s. The entire rectangular fault in divided into 220 subfaults of size 8km x 8km.

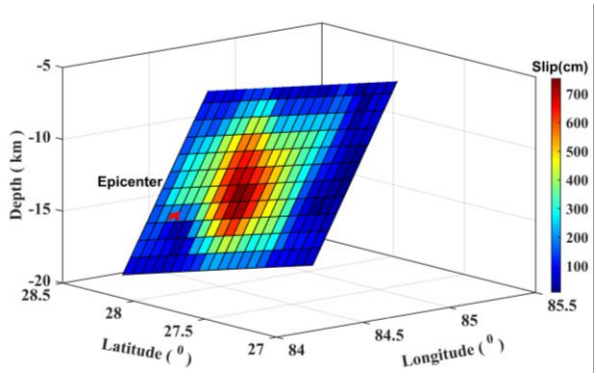

Fig.1. Finite fault slip distribution of the 25th April 2015 Gorkha, Nepal Earthquake

3 MEEMD

The present study introduces an advanced adaptive data analysis technique, namely the multi-dimensional ensemble empirical mode decomposition (Wu *et al.*, [20]) technique, to analysis the spatial variability of the earthquake slips. This MEEMD method has been formulated based on the EMD (Huang [7]) and its more robust version EEMD (Huang and Wu, Wu and Huang [21-22]). In the EMD approach 1-D data, $X(t)$ is decomposed into finite (n) modes of oscillation with certain frequencies called the intrinsic mode functions, IMFs such that

$$X(t) = \sum_{j=1}^{n} IMF_j + R_n(t) \quad (1)$$

where $R_n(t)$ represents the residue of data which can either be a trend (monotonic function with one maxima) or a constant value. The EMD/EEMD approach finds its application in the recently developed MEEMD method. The theory behind MEEMD is to visualize a multi-dimensional dataset as a combination of data in each dimension, which is followed by the application of EEMD to slices of data in each and every dimension and finally reconstructed by combining components of similar scale along each dimension.

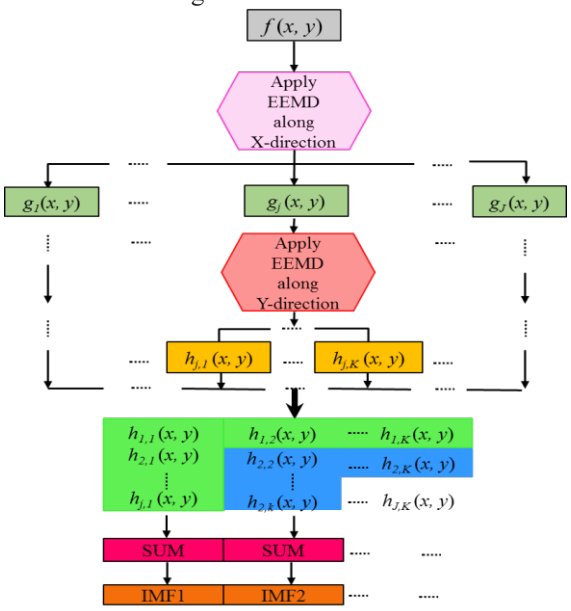

Fig.2. Schematics of MEEMD

A schematic flowchart explaining the MEEMD method for a two-dimensional spatial data such as earthquake slip distribution $f(x, y)$ is shown in figure 2. To start with, we assume the 2-D slip data of Nepal earthquake, $f(x, y)$ as a set of 1-D slices in x-direction (i.e. along the strike). Now, each 1-D slice is decomposed using EEMD resulting in a 2-D pseudo IMF like component $g(x, y)$. This new 2-D data is further decomposed, but this time, the data is considered as a set of 1-D slices in y-direction (i.e. down dip direction) at each location along the x-direction. These 1-D slices of $g(x, y)$ upon EEMD decomposition results in collection of 2-D components of similar scales namely $h(x, y)$. The derived 2-D components are further combined into a reduced set of final IMF components based on the minimal scale combination principle.

3.1 Intrinsic Mode Function

The slip distribution of Nepal earthquake has been decomposed into three dynamic IMFs each evolving around a specific frequency. With the help of these extracted IMFs, one can reconstruct the original slip data as

$$f(x,y)=\sum_{j=1}^{n} IMF_j(x,y)+R(x,y) \quad (2)$$

$R(x, y)$ in equation (2) refers to the residue of the slip data which is similar to $R(t)$ in equation (1). Figure 3 depicts the extracted IMFs along with the residue and slip data. A closer look at the IMFs in figure shows that the number of extremas decreases with increasing hierarchy of IMFs. The statistics of these IMFs are presented in Table 1. The 5x5 correlation matrix clearly shows that there exists a strong correlation between data and IMFs.

Table1. Correlation matrix of IMFs of slip data.

	Data	IMF1	IMF2	IMF3	Trend
Data	1.000	0.200	0.635	0.880	0.900
IMF1		1.000	0.261	0.025	-0.116
IMF2			1.000	0.699	0.294
IMF3				1.000	0.768
Trend					1.000

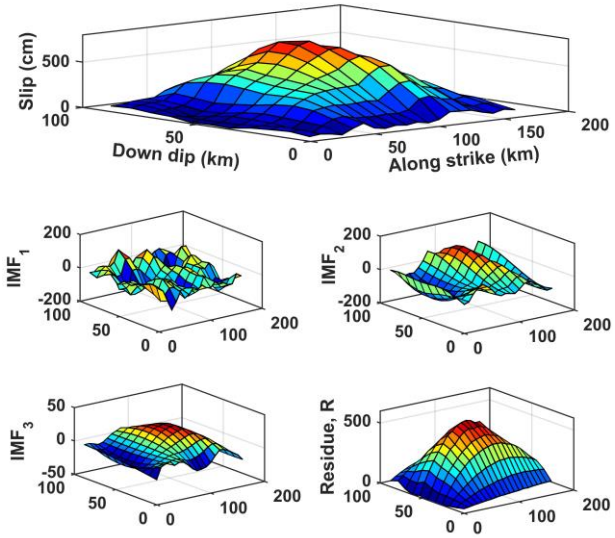

Fig. 3. IMFs and residue of 25th April 2015 Gorkha, Nepal Earthquake

From figure 3, it can also be observed that the residue of the data is positive and slowly varies about the long term average. One may interpret this as a nonstationary component about which the spatial variability of the slip oscillates. This residual component which represents trend of the slip data (as in equation 3) has the highest percentage variance of 74.5% and exhibits the highest correlation of 0.9. On the other hand the fluctuation component of slip which is defined as the summation of all IMFs (as in equation 4) exhibits a percent variance of 25.5%.

$$\text{Trend: } D_T(x,y)=R(x,y) \quad (3)$$

$$\text{Fluctuation: } D_F(x,y)=\sum_{j=1}^{n} IMF_j(x,y) \quad (4)$$

This statistical measure indicates the relative contribution of each component (fluctuation and trend) to the data. It is clearly observed that the fluctuation component characterizes the small scale variability in the data. Contour maps of both these components for the Nepal earthquake are shown in figure 4.

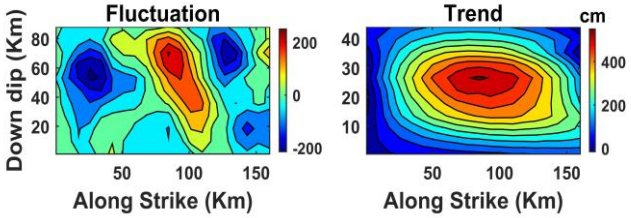

Fig.4. Fluctuation and trend of the slip field shown in figure 1.

The fluctuation component is oscillatory and can be modelled as a random filed. In the second-order analysis, variation of random field at two different locations is characterized either in space by an auto-correlation function (ACF) or in the wave number domain by a power spectral density (PSD). Power spectral density of the slip field and fluctuation are shown in figure 5. Here, the wavenumber ranges between $-\pi/dx$ to π/dx. The spatial frequency content of the fluctuation component is found to be 0-0.2 km^{-1}

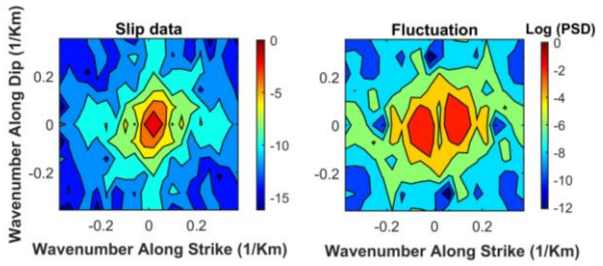

Fig.5. PSD of the slip field and fluctuation component

The article presents a new strategy wherein, one can attempt modelling the slip distribution as a function of fluctuation and trend component instead of modelling the entire slip which is highly erratic.

4 Modelling the fluctuation component

The fluctuation component of the Nepal earthquake as seen in figure 4 is highly complex or random. This erratic nature of the fluctuation component (D_F) can be associated with the randomness observed in ground motion records. The spatial variability of this component can only be modelled as a stationary random field. Assuming the fluctuation component as ergodic, two-dimensional PSD [$D_F(\kappa_x, \kappa_y)$] is obtained from the slip distribution as

$$D_F(\kappa_x,\kappa_y)=\left|\int_{-\infty}^{\infty}\int_{-\infty}^{\infty} D_F(x,y)\ e^{-i\kappa_x x-i\kappa_y y}dxdy\right|^2 \quad (5)$$

where κ_x and κ_y are the spatial wave numbers along the along the strike and dip direction respectively. In the present study, we adopt an exponential random field model to characterize the fluctuation component and is defined as

$$S(\kappa_x,\kappa_y)=\frac{a_x a_y}{(1+k^2)^{3/2}} \qquad (6)$$

where $k=\left(a_x{}^2k_x{}^2+a_y{}^2k_y{}^2\right)^{0.5}$, a_x and a_y denote the correlation length along strike and dip direction respectively. The correlation lengths, a_x and a_y are estimated by minimizing mean square error between the PSD of slip data and PSD computed for the random field model in Equations (6). The deduced correlation length for the Nepal earthquake is estimated as a_x=10 and a_y=15. In Figure 6, the fitted 1D exponential PSD at cross-section k_y =0 and k_x =0 is shown along with the PSD of the data. The best-fit correlation measures are also shown in the same figure for Nepal earthquake, 2015. It can be observed from the figure that the misfit associated with exponential function is negligible. Hence, it can be concluded that the preferred model that is most consistent with the data and which characterizes the complexities of the fluctuation component follows an exponential PSD.

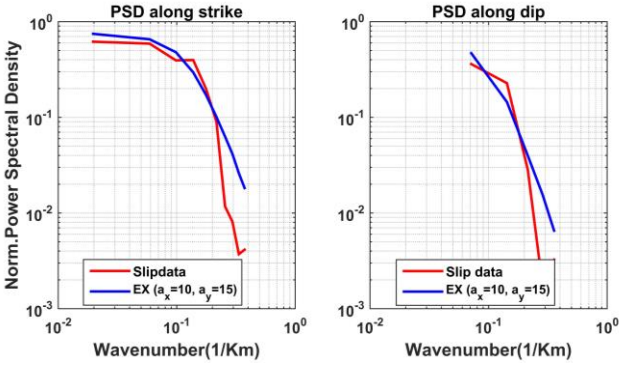

Fig. 6. PSD at the cross sections k_y = 0 and k_x = 0 for the fluctuation component of Nepal event shown in figure 5.

5 Modelling the trend component

The trend represents a positive mean value of the slip field. This nonstationary characteristic of the trend can be modelled by fitting a simple deterministic function. In this study a single elliptic patch model is used to model the trend component. This method has been previously used by Vallée and Bouchon [23] to model entire slip data. In the present, we apply the same technique but, instead of modelling the entire slip data, we try to model only the trend component.

5.1 Single elliptic patch model

As a first step, we estimate the effective rupture area of the trend based on 5%-95% Husid plot which turns out to be 128 x 68 sq. km. This effective rupture patch is shown in figure 7 as a black rectangle. Now, we model this effective rupture area as a single elliptic patch with a constant rise time constant, d_k and rupture velocity, V_r. The precise parameterization of trend component of slip is detailed in Figure 8. A sum of 8 parameters are required to describe this rupture patch. This includes

D -Spatially varying slip distribution of trend
V_r - Rupture velocity
d_k - Rise time
a, b - Geometry of the elliptic patch
D_x, D_z -Shift of the patch centre from the hypocentre of the event
α -Orientation of the ellipse

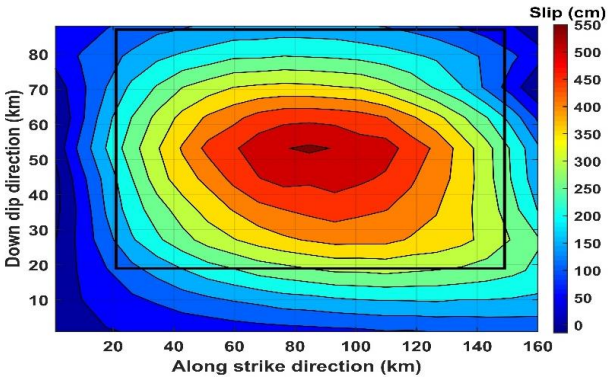

Fig.7. Rupture patch of trend component

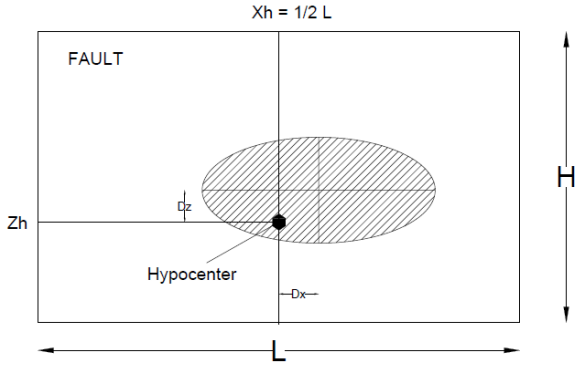

Fig.8. Parameterization for trend modelling of the Nepal earthquake

The parameters a and b are estimated to be 64 km and 34 km respectively. Values of V_r, d_k, D_x and D_z are mentioned in section 2. The orientation of the ellipse, α in taken as 0° as seen in figure 8 for Nepal event. The elliptical perimeter of ellipse is then defined as a collection of points $P_{e,i}$ (i=1,2,3...m) and the nucleation point P_n (x_n,y_n) is given in fault-plane coordinates with origin at the centre of the rupture patch. Now, the slip distribution of the trend, $D(r)$ along line i from P_n to each point $P_{e,i}$ ($x_{e,i}$, $y_{e,i}$) on the perimeter of the ellipse can be expressed as

$$D(r)=\frac{D_p}{1-D_{\min}}(e^{-k_i r^2}-D_{\min}), \qquad 0\le r\le R_i \qquad (7)$$

where,

D_p – Max slip
D_{min} – 0.1 D_p
k_i – Exponential decay coefficient
R_i – Distance from r=0 to r=R_i

Equation (7) yields continuous, spatially smooth pseudo-Gaussian slip distribution of the trend on the elliptical rupture patch. Rupture initiates at P_n and propagates radially at rupture velocity V_r. Boundary conditions (equation 8) are satisfied to estimate slip, $D(r)$. We finally superimpose $D(r)$ on a Cartesian co-ordinate system as D_T (x, y). The estimated slip distribution of trend is shown in figure 9.

$$BC1: \quad D(r=0) = D \text{ and } \frac{d}{dr}D(r=0) = 0, \qquad (8)$$
$$BC2: \quad D(r=R) = 0$$

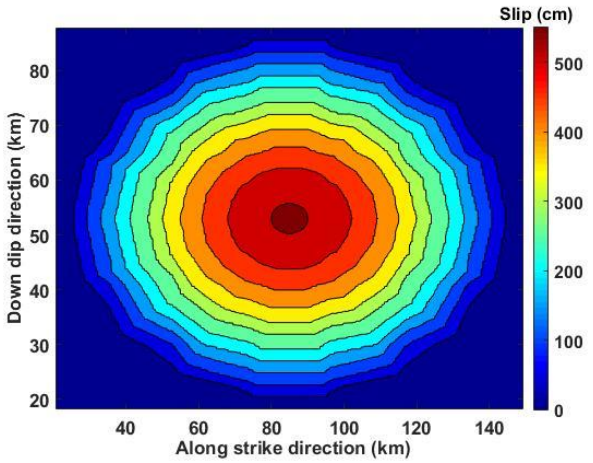

Fig. 9. Estimated trend component

6 Simulated slip field

The final slip field can be obtained as a weighted sum of the fluctuation and trend components. In this case, explained variance of each component is taken as weightage. Figure 10 shows the final simulated slip field for the 25th April 2015 Nepal earthquake. The simulated slip field is in good agreement with original slip data shown in figure 1. The total moment of the simulated slip is comparable to total moment of the data.

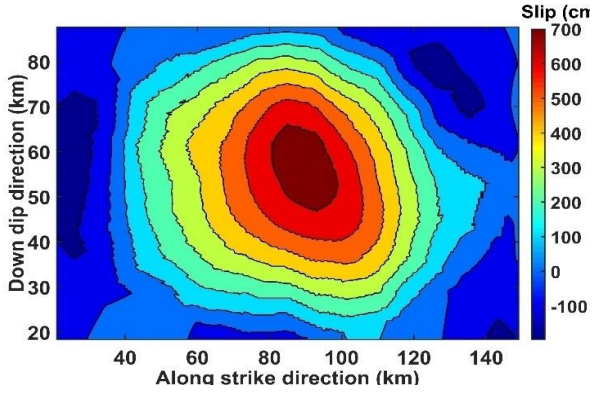

Fig. 10. Simulated slip field

7 Simulation procedure for a hypothetical future event

1. Fix the focal mechanism (strike, dip, rake)
2. Assume faulting-style (Strike-slip, Reverse, Normal)
3. Choose the Moment magnitude, M_w of the potential earthquake
4. Determine the moment magnitude, M_0 from $M_w=2/3\ \log_{10}(M_0)-10.7$
5. Determine the fault length L, fault width W, mean slip d and σ_d from scaling relations
6. Estimate correlation lengths a_x, a_y from scaling relations for an exponential random field.
7. Simulate fluctuation component as an exponential random field from the spectral representation method of Shinozuka and Deodatis [24] or Fourier integral method of Pardo-Igu´zquiza and Chica-Olmo [25] using the estimated correlation lengths
8. Simulate tend component as a single patch rupture model using the parameters a, b, α, D_p for a given event.
9. Obtain the final random field as a weighted sum of fluctuation and trend component.
10. Fix hypocentre of the event.

An ensemble of slip fields can be simulated using the proposed methodology. The simulated slip field from this approach finds its application in the synthesis of several realizations of accelerograms using any of the analytical approaches.

7 Discussion and conclusion

A novel approach to model spatial complexity of slip on the fault plane using MEEMD technique has been explored in this article. The decomposition of the fault slip into IMFs brings out certain interesting features of the slip distribution of Nepal earthquake. The most interesting feature that has been observed is that, MEEMD sorts the spatial frequency content of the slip distribution into a finite set of IMFs with the highest and lowest frequency corresponding to the first IMF and trend, respectively. One can try modelling the randomness associated with each IMF separately, however, this may lead to an increase in the number of model parameters whereby reducing the efficiency of the developed model. To overcome this limitation, in the present study, it is proposed that the slip field can be modelled as a combination of stationary random field (fluctuation) and a nonstationary trend. Given a particular fault and magnitude, the proposed model can handle uncertainties in the slip distribution. The developed stochastic source model together with seismological method or Spectral Finite Element Method, can be used to synthesize an ensemble of ground motion time histories for any future earthquake and for regions lacking strong motion data. Further, randomness in the simulated time histories can be attributed to the fluctuation component while peak ground displacement and peak ground residual displacement being associated with the trend term. Another advantage with the developed model is that the estimated slip field from this approach finds its real time application in generation of seismic or tsunami hazard maps.

8 Reference

1. Somerville, P., Irikura, K., Graves, R., Sawada, S., Wald, D., Abrahamson, N., Iwasaki, Y., Kagawa, T., Smith, N., Kowada, A. (1999). Characterizing Crustal Earthquake Slip Models for the Prediction of Strong Ground Motion. *Seismological Research Letters* **70**(1), 59-80.
2. Mai, P. M. and Beroza, G. C. (2002). A spatial random field model to characterize complexity in earthquake slip. *Journal of Geophysical Research* **187**(11), 1-28.
3. Lavall*ée*, D., Liu, P. and Archuleta, R. J. (2006). Stochastic model of heterogeneity in earthquake spatial distribution. *Geophysical Journal International* **165**, 622–640.
4. RaghuKanth, S. T. G. and Iyengar, R. N. (2009). Engineering source model for strong ground motion. *Soil Dynamics and Earthquake Engineering* **29**, 483-503.
5. RaghuKanth, S. T. G. (2010). Intrinsic mode functions of earthquake slip distribution. *Advances in Adaptive Data Analysis* **2**(2), 193–215
6. Raghukanth, S.T.G. and Sangeetha, S. (2014), A stochastic model for earthquake slip distribution of large events, *Geomatics, Natural Hazards and Risk,* DOI:10.1080/19475705.2014.941418
7. Huang, N. E., Shen, Z., Long, S. R., Wu, C. M., Shih, H. H., Zheng, Q., Yen, N. C., Tung, C. C., and Liu, H. H. (1998). The empirical mode decomposition and the Hilbert spectrum for nonlinear and non-stationary time series analysis. *Proceedings of the Royal Society London* **454**, 903–995.
8. Huang, N. E., Chern, C. C., Huang, K., Salvino, L. W., Long, S. R., and Fan, K. L. (2001). A new spectral representation of earthquake data: Hilbert spectral analysis of station TCU129, Chi-Chi, Taiwan, 21 September 1999. *Bulletin of the Seismological Society of America* **91**(5), 1310–1338.
9. Loh, C. H., Wu, T. C. and Huang, N. E. (2001). Application of the empirical mode decomposition-Hilbert spectrum method to identify near-fault ground-motion characteristics and structural responses. *Bulletin of the Seismological Society of America* **91**, 1339–1357.
10. Zhang, R. R., Ma, S., Safak, E. and Hartzell, S. (2003). Hilbert-Huang Transform Analysis of Dynamic and Earthquake Motion Recordings. *Journal of Engineering Mechanics* **129**(8), 861– 875.
11. Raghukanth, S.T.G. and Sangeetha, S. (2013), Empirical mode decomposition of earthquake accelerograms, *Advances in Adaptive Data Analysis* **4**(3). DOI: 10.1142/S1793536912500239
12. Mallikarjuna, C. and Raghukanth, S. T. G. (2010). Forecasting the air traffic for north-east indian cities, *Advances in Adaptive Data Analysis* **2**(1),1-16
13. Hayes, G.P., Briggs, R.W., Barnhart, W.D., Yeck, W.L., McNamara, D.E., Wald, D.J., Nealy, J.L., Benz, H.M., Gold, R.D., Jaiswal, K.S., Marano, K., Earle, P.S., Hearne, M.G., Smoczyk, G.M., Wald, L.A., Samsonov, S.V., 2015. Characterization of the 2015 M_w 7.8 Nepal (Gorkha) earthquake sequence and its seismotectonic context. *Seismological Research Letters* **86**(6), 1557–1567.
14. Yagi, Y., and Okuwaki, R. (2015). Integrated seismic source model of the 2015 Gorkha, Nepal, earthquake, *Geophysical Research Letters* 42, 6229–6235.
15. Lay, T., Ye, L., Koper, K.D., Kanamori, H., (2016). Assessment of teleseismically determined source parameters for the April 25, 2015 M_w7.9 Gorkha, Nepal earthquake and the May 12, 2015 M_w 7.2 aftershock. *Tectonophysics* 714–715, 4–20.
16. Tung, S., and T. Masterlark (2016), Coseismic slip distribution of the 2015 M_w 7.8 Gorkha, Nepal, earthquake from joint inversion of GPS and InSAR data for slip within a 3-D heterogeneous Domain, *Journal of Geophysical Research Solid Earth* 121, 3479–3503.
17. Yue, H., Simon, M., Duputel, Z., Jiang, J., Fielding, E., Liang, C., Owen, S., Moore, A., Riel, B., Ampuero, J.P., Samsonov, S.V. (2016). Depth varying rupture properties during the 2015 M_w 7.8 Gorkha (Nepal) earthquake. *Tectonophysics* 714–715 (2017) 44–54
18. Zhang, L., Lia, J., Liao, W., Wang, Q. (2016). Source rupture process of the (2015) Gorkha, Nepal M_w7.9 earthquake and its tectonic implications. *Geodesy and geodynamics* 7(2) , 124 -131
19. McNamara, D.E., Yeck, W.L., Barnhart, W.D., Schulte-Pelkum,V., Bergmane.,L., Adhikarid, L.B., Dixit, A., Hough, S.E., Benza, H.M., .Earlea, P.S. (2016).Source modeling of the 2015 M_w 7.8 Nepal (Gorkha) earthquake sequence: Implications for geodynamics and earthquake hazards. *Tectonophysics* 714–715, 21–30
20. Wu, Z., Huang, N. E., and Chen, X. (2009). The multi-dimensional ensemble empirical mode decomposition method. *Advances in Adaptive Data Analysis* 1, 339–372.
21. Huang, N. E., and Wu, Z. 2008. A review on Hilbert-Huang transform: Method and its applications on geophysical studies. *Reviews of Geophysics* 46, RG2006, doi: 10.1029/2007RG000228.
22. Wu, Z., and Huang, N. E. (2009). Ensemble empirical mode decomposition: A noise-assisted data analysis method. *Advances in Adaptive Data Analysis* 1, 1–41
23. Vallee, M. and Bouchan, M. (2004) .Imaging coseismic rupture in far Þeld by slip patches. *Geophysical Journal International* **156,** 615-630.
24. Shinozuka, M., and Deodatis, G. (1998). Stochastic process models for Earthquake source. *Probablistic Engineering Mechanic*s **3**(3), 114-123.
25. Pardo-Igu´ zquiza, E., Chica-Olmo, M., (1993). The Fourier integral method—an efficient spectral method for simulation of random fields. *Mathematical Geology* **25** (2), 177–217.